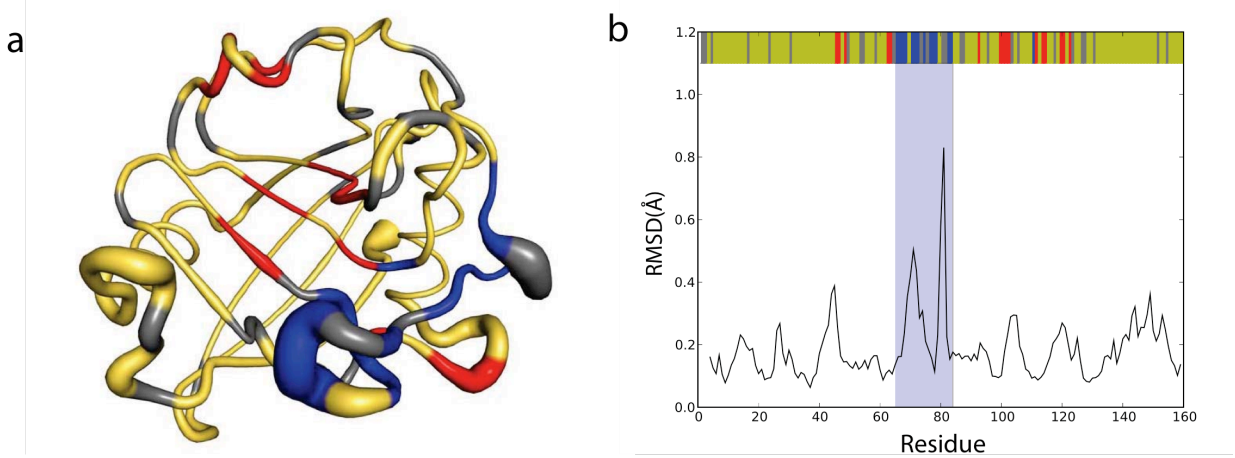

Supplementary Figure 1. Crystal structures of CypA differ in loops but not in residues coupled to the active site. Backbone RMSD from a structural superposition of 48 CypA crystal structures in **a**, sausage representation of with thickness is proportional to backbone RMSD and **b**, as a function of residue number. The color-coding used is based on previous NMR relaxation dispersion experiments (ref. 4): group I (red), group II (blue), residues that do not display R_{EX} (yellow), and prolines or unresolved amides (grey). Backbone differences of group II residues, but not group I residues, explain the different chemical environments of the major and minor states inferred through relaxation dispersion NMR. Forty-eight CypA structures, some of the free enzyme and some with ligands bound, were superimposed using Theseus[41]: (Structure_chain)--1ak4_A, 1cwc_A, 1m63_C, 1oca_A, 2cpl_A, 1awq_A, 1cwf_A, 1m9c_A, 1rmh_A, 2cyh_A, 1awr_A, 1cwh_A, 1m9d_A, 1vbs_A, 2rma_A, 1aws_A, 1cwi_A, 1m9e_A, 1vbt_A, 2rmb_A, 1awt_A, 1cwj_A, 1m9f_A, 1w8l_A, 3cyh_A, 1awu_A, 1cwk_A, 1m9x_A, 1w8m_A, 3cys_A, 1awv_A, 1cwl_A, 1m9y_A, 1w8v_A, 4cyh_A,1bck_A, 1cwm_A, 1mf8_C, 1ynd_A, 5cyh_A,1cwa_A, 1cwo_A, 1mik_A, 1zkf_A,1cwb_A, 1fgl_A, 1nmk_A, 2alf_A.

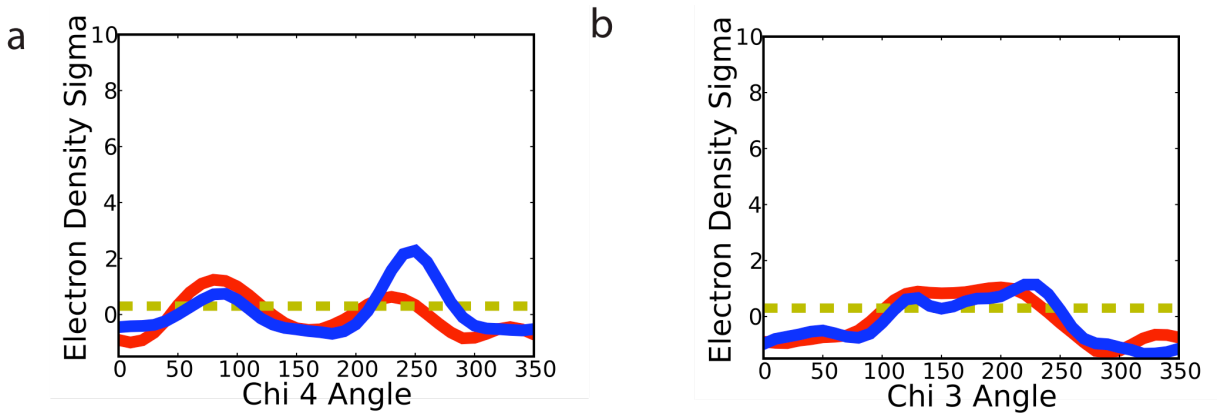

Supplementary Figure 2. Ringer identifies discrete side-chain heterogeneity for active-site residues in the cryogenic (100 K), 1.2-Å-resolution electron density of wild-type CypA. a, Arg55 χ4 and **b**, Met61 χ3. At room temperature, additional peaks for these and neighboring residues were present in the electron density from data collected at both cyrogenic (blue) and room temperature (red) (see also Fig. 1). These data reinforce the point that some CypA residues are polymorphic at both room and cryogenic and others are only polymorphic at room temperature.

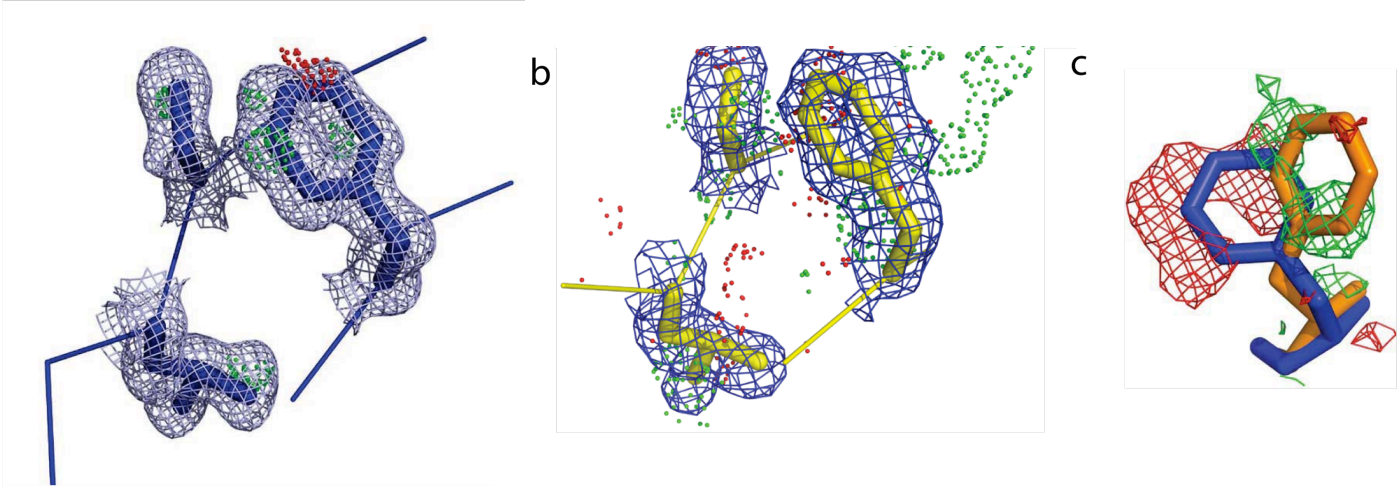

Supplementary Figure 3. The alternate CypA conformations are present at room temperature, but not cryogenic temperatures. a, Electron-density maps calculated using X-ray data collected at 100 K define unique conformers of Leu98, Ser99 and Phe113. 2Fo-Fc electron density (blue mesh; 1σ); positive (green) and negative (red) Fo-Fc difference density (3σ). The lack of difference density surrounding Phe113, in contrast to the room temperature data shown in Figure 1b, suggests a unique conformation best fits the electron density. 2Fo-Fc electron density around the main chain and the surrounding residues was omitted for clarity. **b,** The alternate conformation is unaffected by the cryoprotectant, 15% xylitol. 2Fo-Fc electron density (blue mesh; 1σ); positive (green) and negative (red) Fo-Fc difference density (3σ) calculated from a 1.45-Å-resolution data set collected at room temperature with 15% xylitol present. The difference density pattern is similar to the high-resolution room temperature electron density shown in Figure 1b obtained in the absence of xylitol. **c,** An isomorphous difference map ($F_{room\_temperature} - F_{cryogenic}$ and phases from the model using the data obtained at 100 K) reveals directly the shift to the minor state at room temperature. Negative difference density (red, 2.5σ) surrounds the major conformation and positive difference density (green, 2.5σ) reveals the hidden minor state.

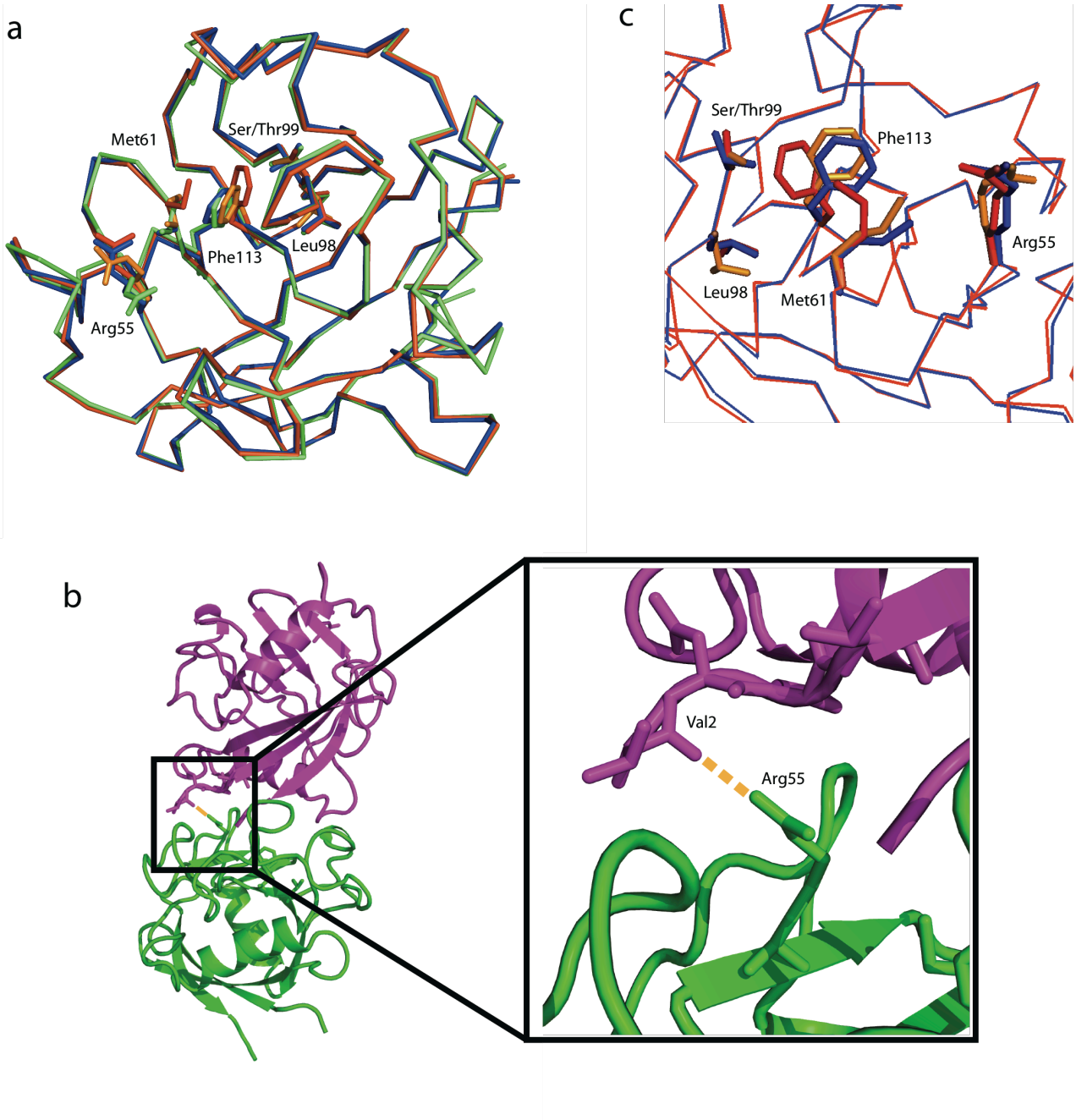

Supplementary Figure 4. The structure of Ser99Thr CypA contains features of the minor conformation of wild-type enzyme. a, Ribbon overlay of the structures of wild-type CypA in the orthorhombic crystal form (backbone in orange-red, major-state side chains in red, minor-state side chains in orange), the Ser99Thr mutant trigonal form (green), and Ser99Thr mutant orthorombic form (blue) with the side-chains Arg55,

Met61, Leu98, Ser/Thr99 and Phe113 shown in sticks. **b,** Arg55 adopts a different rotamer in the trigonal crystals due to crystal contacts. The Arg55 guanidino group is 3.1 Å (orange line) from the carbonyl oxygen of Val2 of the symmetry-related molecule (magenta). **c,** In the isomorphous orthorhombic crystal forms, Arg55, Phe113 and Thr99 (Ser99 in the wild-type enzyme) adopt similar conformations in the Ser99Thr mutant (blue) and the minor conformational substate of wild-type CypA (orange).

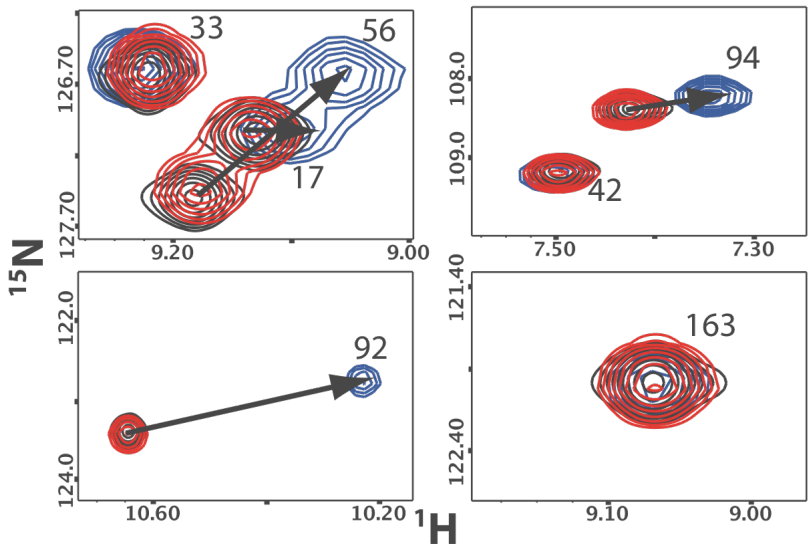

Supplementary Figure 5. **Additional residues show that the Ser99Thr mutation shifts the equilibrium toward the minor wild-type conformation.** Linear amide chemical shift changes (arrows) between wild-type (black), Lys82Ala (red) and Ser99Thr (blue) CypA reflect the inversion of the major/minor equilibrium due to the Ser99Thr mutation. Residue 163 is shown as a representative residue that does not differ in chemical shift between the major and minor state.

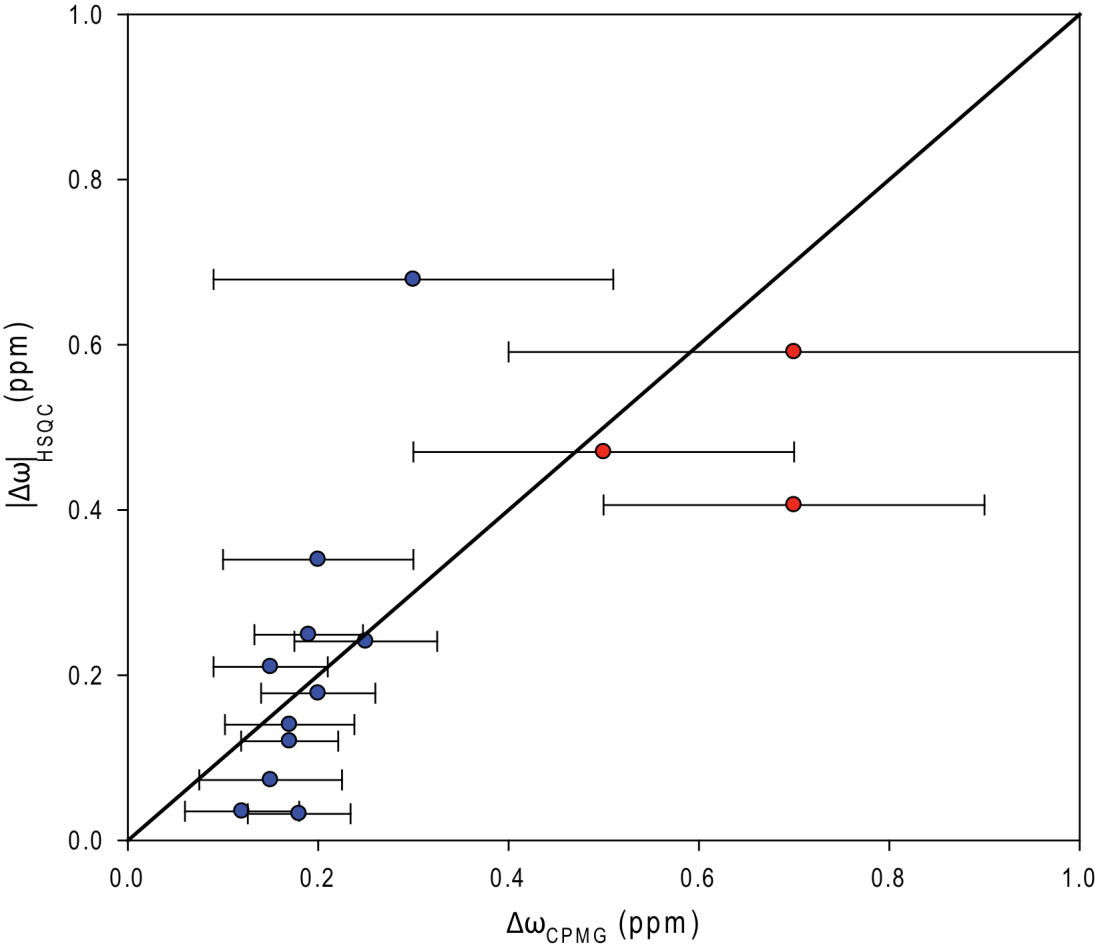

Supplementary Figure 6. Evidence for inversion of minor/major equilibrium in Ser99Thr CypA relative to wild-type CypA. Correlation of 13C methyl (blue) and 15N backbone (red) chemical shift differences between Ser99Thr and wild-type CypA, measured from HSQC spectra, and the chemical shift differences calculated from the corresponding wildtype CPMG relaxation dispersion data fitted to the full Carver Richards equation at 10 ºC[4]. The CPMG data[4] were fit using an improved fitting protocol (see methods). The large percentage uncertainties originate in the very small amplitudes of dispersion (between 0.5 and 1.5 Hz).

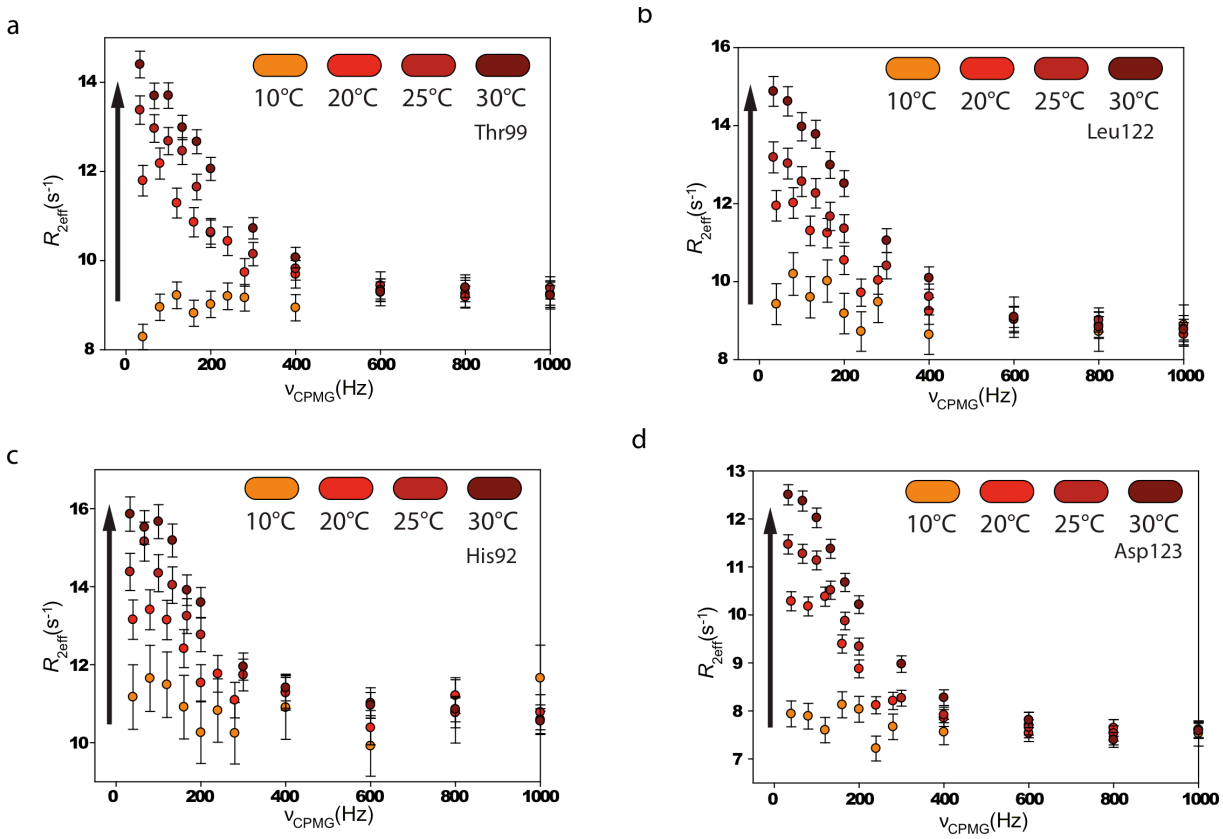

Supplementary Figure 7. **Group I residues in the Ser99Thr mutant undergo dynamics in the slow NMR time regime.** Temperature dependence of CPMG ^{15}N NMR relaxation data for group I residues, which couple to the active site: **a,** Thr99, **b,** Leu122, **c,** His92, and **d,** Asp123 in Ser99Thr CypA. The Ser99Thr mutation impedes group I conformational dynamics, shifting the motions collectively into the slow NMR time regime. The characteristic increase of R_{EX} with temperature (arrows) demonstrates that $R_{EX} \sim k_1$, the rate constant for the efflux from the major state. Curves were normalized as in Fig. 3d.

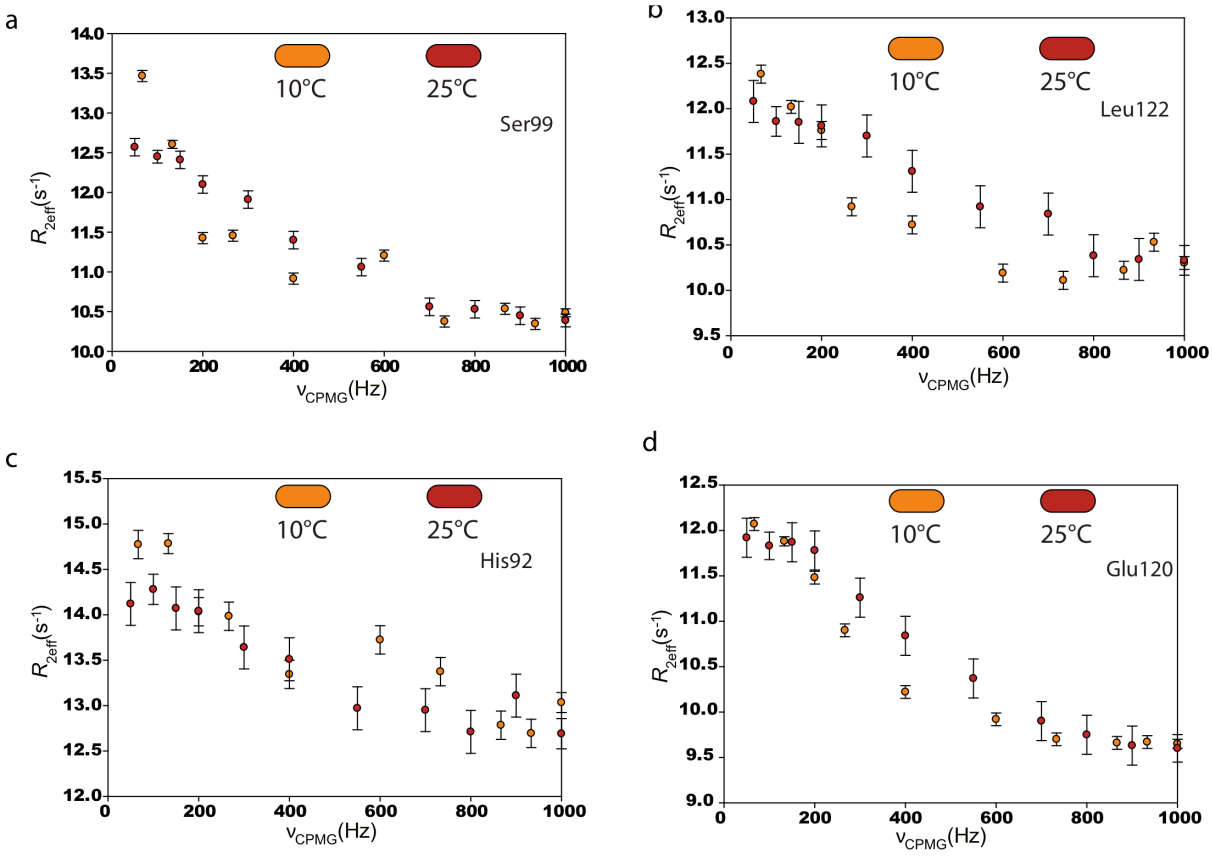

Supplementary Figure 8. **Group I residues in wild-type CypA undergo dynamics in the intermediate to fast NMR time regime.** Temperature dependence of CPMG ^{15}N NMR relaxation data for group I residues **a,** Ser99, **b,** Leu122, **c,** His92 and **d,** Glu120 in wild-type CypA do not reveal the temperature dependence of group I conformational dynamics as seen in Ser99Thr CypA, revealing that motions occur in the intermediate/fast NMR time regime. Curves were normalized as in Fig. 3d.

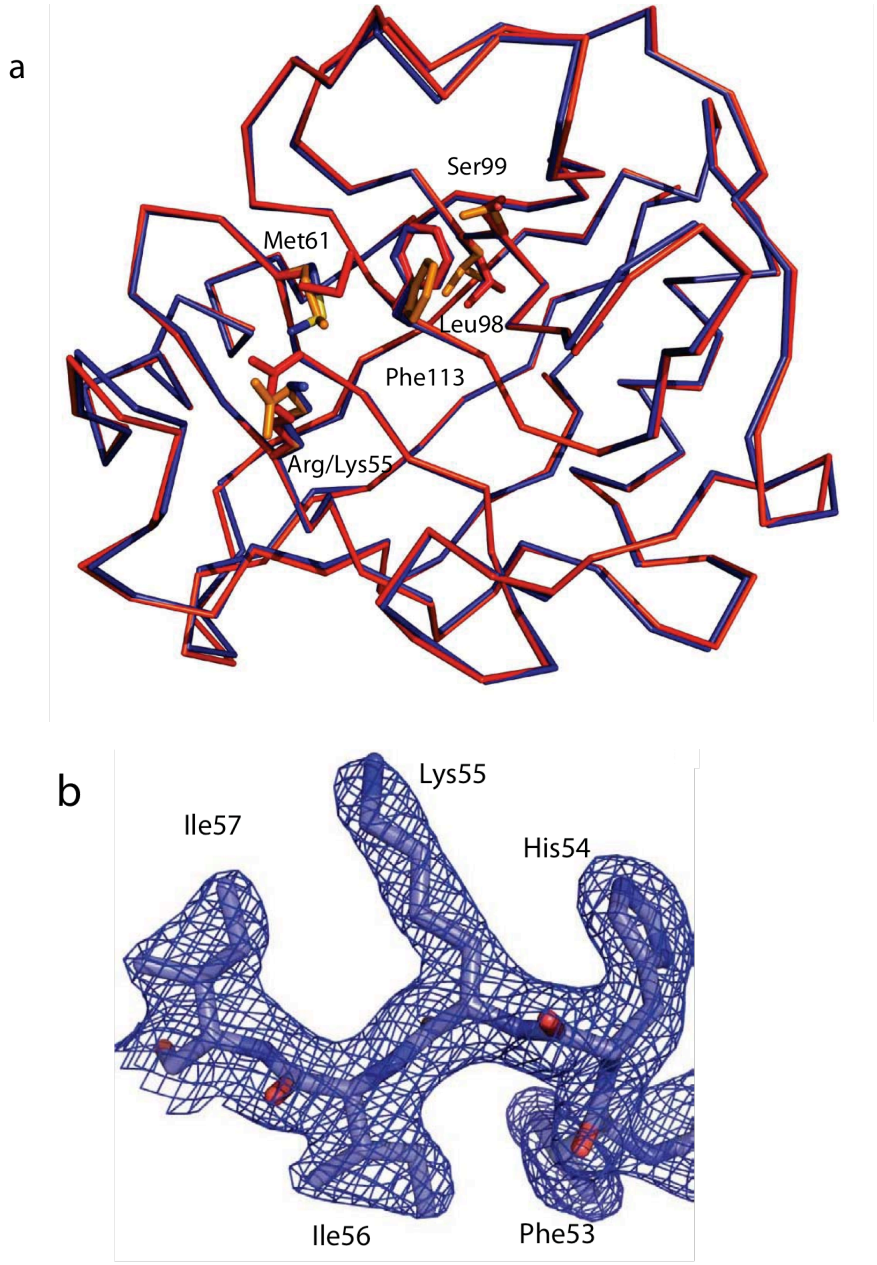

Supplementary Figure 9. X-ray structure of the chemically impeded Arg55Lys mutant. a, Arg55Lys CypA (blue) adopts a global structure similar to the wild-type enzyme (backbone in orange-red, major state side chains in red, minor state side chains in orange). **b,** 2Fo-Fc electron density (1σ, 2.4 Å resolution, 100 K data collection temperature) for Lys55 and the neighboring residues. This resolution is not sufficient to monitor alternate conformations by Ringer.

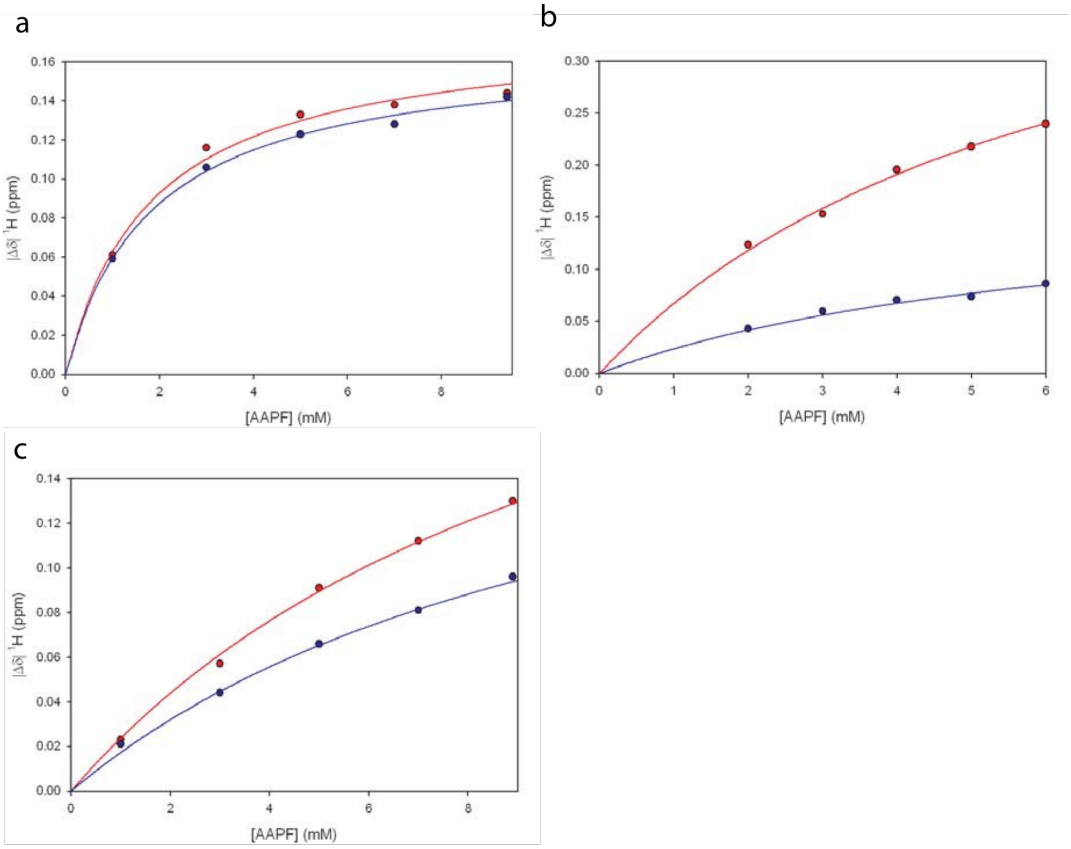

Supplementary Figure 10. NMR measurements of the affinity of CypA variants for the substrate peptide, N-succinyl-Ala-Ala-Pro-Phe-p-nitroanilide (AAPF).

Representative chemical-shift changes for AAPF binding to **a**, wild-type, **b**, Ser99Thr, and **c**, Arg55Lys CypA derived from 1H-15N HSQC spectra collected at 6 ºC. Changes in proton chemical shift (circles) as a function of peptide concentration were fit for single-site binding (lines). Residues 63 (a, red) and 100 (a, blue), 52 (b, red) and 81 (b, blue), and 101 (c, red) and 102 (c, blue) were among those used in global fits of KD for each variant. The set of residues used to determine the KD's differed for each CypA variant due to changes in resonance overlap. The fitted values are observed KD's (see supplementary table 4) representing population-averaged values for the cis- and trans-isomers.

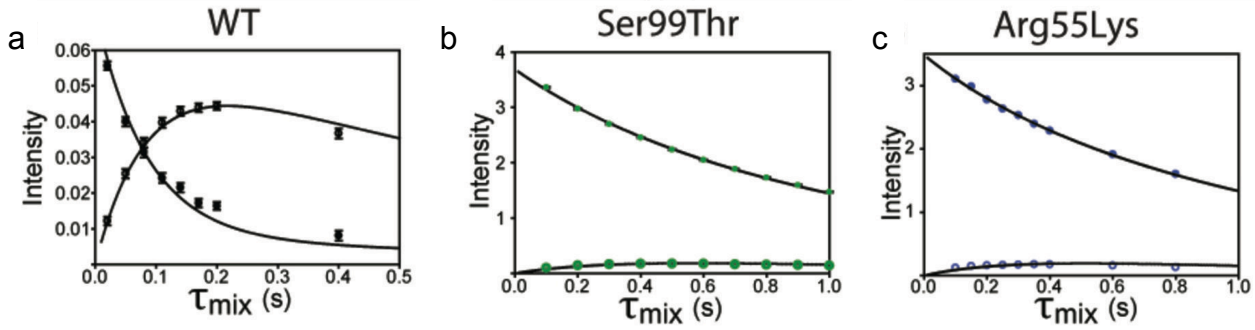

Supplementary Figure 11. Quantification of catalytic activity of wild-type, Ser99Thr and Arg55Lys mutant forms of CypA. Decay and buildup curves from ^{1}H-^{1}H NOE-exchange spectra collected with different mixing times[21] of the *cis*-auto peak of Ala2 and the corresponding exchange peak in the presence of **a,** 2.2 μM wild-type or the *trans*-auto peak of Pro3 and the corresponding exchange peak in the presence of **b,** 92 μM Ser99Thr and **c,** Arg55Lys.

Supplementary Table 1. Data collection and refinement statistics.

	WT-Cryo	WT-Room	S99T-Room	S99T-trigonal-cryo	S99T-orthorombic-cryo	R55K-cryo
Space Group	$P2_12_12_1$	$P2_12_12_1$	$P3_221$	$P3_221$	$P2_12_12_1$	$P3_221$
Cell Dimensions a, b, c (Å)	42.4, 51.7, 88.6	43.1, 52.6, 89.3	60.4, 60.4, 95.5	59.7, 59.7, 94.3	42.5, 52.1, 89.1	64.2, 64.2, 93.6
Resolution (Å)	50-1.25 (1.29-1.25)	50-1.39 (1.44-1.39)	50-1.55 (1.61-1.55)	50-1.65 (1.71-1.65)	50-2.31 (2.39-2.31)	50-2.42 (2.51-2.42)
R_{sym}	0.042 (0.564)	0.049 (0.525)	0.102 (0.441)	0.077 (0.410)	0.092(0.193)	0.131 (0.572)
I/σ	38.3 (3.6)	33.8 (1.9)	21.0 (3.0)	24.8 (2.9)	11.8 (3.7)	16.4 (3.9)
Completeness (%)	99.7 (99.1)	99.2 (92.3)	90.8 (55.0)	99.2 (92.1)	87.3(48.4)	100 (100)
Redundancy	7.4 (7.1)	7.4 (2.9)	13.3 (5.6)	7.4 (4.2)	3.3 (1.9)	9.8 (9.3)
Reflections	54749 (5385)	41145 (3767)	27237 (1609)	23875 (2180)	7936 (430)	8900 (853)
R_{work}/R_{free} (%)	12.9/14.9	12.2/16.0	10.7/14.8	14.7/17.6	17.6/24.7	17.7/23.6
No. atoms						
• Protein	2740	3040	2447	2447	2482	2477
• Water	269	132	119	218	95	59
Average B-factors						
• Protein ($Å^2$)	13.66	23.68	20.14	15.24	27.61	33.96
• Water ($Å^2$)	28.91	37.28	33.34	29.79	32.15	34.83
R.M.S deviations						
• Angles (°)	1.307	1.264	1.310	1.445	1.569	1.762
• Bonds (Å)	0.010	0.011	0.011	0.014	0.016	0.019
Beamline	SSRL 9-1	ALS 12.3.1	ALS 12.3.1	ALS 8.3.1	ALS 8.3.1	ALS 8.3.1
Data collection temperature	100K	288K	288K	100K	100K	100K
PDB code	3K0M	3K0N	3K0O	3K0P	3K0Q	3K0R

The highest resolution shell is shown in parentheses.

Supplementary Table 2: Aromatic 3-bond *J* (^3J) couplings in CypA

	WT		Ser99Thr	
Residue	$^3J_{C'C_\gamma}$ (Hz)	$^3J_{NC_\gamma}$ (Hz)	$^3J_{C'C_\gamma}$ (Hz)	$^3J_{NC_\gamma}$ (Hz)
Phe25	3.62 ± 0.11	0.78 ± 0.29	3.75 ± 0.09	0.75 ± 0.27
Tyr79	3.31 ± 0.12	1.01 ± 0.32	3.39 ± 0.08	0.67 ± 0.34
Phe88	3.64 ± 0.14	0.77 ± 0.31	3.28 ± 0.16	0.54 ± 0.36
His92	3.64 ± 0.18	0.97 ± 0.36	3.91 ± 0.17	1.23 ± 0.33
Phe113	**1.12 ± 0.63**	**0.91 ± 0.32**	**2.77 ± 0.23**	**0.81 ± 0.41**
Phe145	3.35 ± 0.12	0.89 ± 0.24	3.49 ± 0.09	0.25 ± 0.76

^3J couplings between backbone atoms and $C\gamma$[29], showing a change in Phe113 rotameric state (highlighted in bold) between WT and Ser99Thr. Only residues with full data for both variants are shown. All experiments were performed at 25 ˚C, except WT Phe113 $^3J_{C'C_\gamma}$, taken at 5 ˚C due to resonance overlap.

Supplementary Table 3: Relaxation dispersion parameters for Ser99Thr CypA

Residue	10˚C R_{EX} (/s)[a]	20˚C R_{EX} (/s)[a]	25˚C R_{EX} (/s)[a]	30˚C R_{EX} (/s)[a]	α (25˚C)[b]
90	1.7 ± 0.9	2.2 ± 0.4	2.1 ± 0.4	2.1 ± 0.3	0.3
92	0.8 ± 1.1	2.9 ± 0.7	4.1 ± 0.6	5.2 ± 0.5	0.0
99	N/D[c]	3.2 ± 0.5	4.3 ± 0.4	5.5 ± 0.4	0.0
113	1.1 ± 0.7	2.8 ± 0.5	3.9 ± 0.4	3.6 ± 0.4	0.1
114	1.4 ± 0.7	2.2 ± 0.5	2.0 ± 0.4	N/D[c]	0.5
119	0.8 ± 0.3	2.9 ± 0.2	3.3 ± 0.2	2.8 ± 0.2	0.9
120	0.9 ± 0.4	3.3 ± 0.5	4.6 ± 0.3	5.7 ± 0.4	0.3
122	0.6 ± 0.7	3.4 ± 0.3	4.7 ± 0.5	6.4 ± 0.5	0.0
123	0.6 ± 0.4	3.1 ± 0.5	4.3 ± 0.3	5.4 ± 0.3	0.0
126	N/D[c]	3.8 ± 0.5	4.0 ± 0.4	4.4 ± 0.4	0.2
127	0.8 ± 0.4	3.2 ± 0.9	5.5 ± 1.0	6.9 ± 1.1	0.0
128	1.5 ± 2.0	2.1 ± 1.1	5.1 ± 1.1	7.6 ± 1.2	0.0
k_1 (R_{EX})[d]	1.0 ± 0.4	2.9 ± 0.5	4.0 ± 1.1	4.7 ± 2.0	
k_1 (fit)[e]	1.00 ± 0.20	2.96 ± 0.18	4.98 ± 0.65	8.22 ± 0.49	

Relaxation parameters for group I residues in Ser99Thr CypA that were used in global fitting. [a] apparent R_{EX} estimated from relaxation-dispersion curves at 600 MHz. [b] α[19] calculated from apparent R_{EX} at 800, 600, and 500 MHz. [c] Not determined due to resonance overlap or excessive noise. [d] k_1 calculated as average of apparent R_{EX} of all group I residues. [e] k_1 fitted globally from group I relaxation-dispersion data using the full Carver-Richards equation. It is apparent that above 25˚C, the exchange moves form the slow NMR time regime to the intermediate NMR time regime.

Supplementary Table 4. Kinetic constants for the reaction of CypA variants with the subtrate N-succinyl-Ala-Ala-Pro-Phe-p-nitroanilide (AAPF).

	k_{cat}/K_M ($s^{-1}M^{-1}$) [a]	K_D (mM) [b]	k_{cat}^{isom} (s^{-1}) [c]
WT	$1.4x10^7$+/-0.1 $x10^7$	1.8+/-0.14	$1.3x10^4$+/-800
Ser99Thr	$4.5x10^4$ +/-$0.4x10^4$	6.7+/-0.8	1.9 $x10^2$+/-20
Arg55Lys	$1.4x10^4$+/-$0.2x10^4$	11.3+/-2.5	3.8 $x10^2$+/-90

(mean +/- s.d.)

[a]kcat/KM for the cis to trans direction determined from the coupled chymotrypsin assay[20] at 10˚C. [b] determined from NMR titration data at 6˚C. [c] determined from the NOESY exchange spectra at 6˚C using the K_d from[b].